Influence of substrate pore structure and nanolime particle size on the effectiveness of nanolime treatments

OTERO, Jorge, STARINIERI, Vincenzo <http://orcid.org/0000-0002-7556-0702> and CHAROLA, AE

Published version

OTERO, Jorge, STARINIERI, Vincenzo and CHAROLA, AE (2019). Influence of substrate pore structure and nanolime particle size on the effectiveness of nanolime treatments. Construction and Building Materials, 209, 701-708.

Influence of substrate pore structure and nanolime particle size on the effectiveness of nanolime treatments

J. Otero[a,b*], V. Starinieri[a], A. E. Charola[c]

[a] *Materials and Engineering Research Institute, Sheffield Hallam University, Sheffield, S1 1WB, UK*

[b] *Getty Conservation Institute, The J. Paul Getty Trust, Los Angeles, CA 90049, US*

[c] *Museum Conservation Institute, Smithsonian Institution, Washington DC, USA*

* corresponding author: Tel: +44 1142253500; Fax: +44 114 225 3501; Jotero@getty.edu; jorge.otero.h@gmail.com

KEYWORDS: Nanolime; Microstructure; Porosity; Consolidation; Stone; Nanoparticles

Abstract. Nanolime is a promising consolidation treatment for the conservation of historic structures thanks to its high compatibility with carbonate-based substrates. Nanolime products can effectively reduce the porosity and restore the mechanical properties of treated surfaces. Whilst the popularity of nanolime has been growing, its consolidation mechanism still needs to be fully understood when applied to porous substrates. The aim of this paper is to determine the influence of nanolime particle size and substrate pore structure on the effectiveness of nanolime treatments. Results suggest that nanolime products with larger particle size tend to close predominantly large sized pores, while nanolime with smaller particle size tends to fill both large and small pores equally. These results suggest that for a consolidation treatment, the nanolime product must be chosen taking into consideration the substrate pore structure.

1. Introduction

One of the most relevant conservation principles, promulgated by the Athens Charter for the Restoration of Historic Monuments in 1931 [ICOMOS 1931], states that historic objects or structures with significant value (artistic, cultural or historical) must be, whenever possible, restored and preserved. Calcareous limestones are important construction materials used in Cultural Heritage around the world throughout history. These substrates are

susceptible to several weathering processes (e.g. freeze-thaw, salt damage, dissolution, acidic attack, etc) which lead structures to lose some of their original properties [Doehne and Price, 2009].

Consolidation products are used to restore the materials original properties. These consolidants must be physico-chemically compatible with the matrix and should restore its mechanical properties [ICOMOS, 1964]. In recent years the most used consolidating products are silica-precursor consolidants (e.g. TEOS or MTMOS). These products are used in restoration treatments thanks to their ease of application, good penetration and immediate strength enhancement [Wheeler, 2005]. However, in the case of calcareous substrates, the low physical and mechanical compatibility of silica-precursor consolidants with the mineral substrate can cause cracks and significant damage in the long-term [Wheeler, 2005; Wheeler, 2008; Ferreira-Pinto and Delgado-Rodrigues, 2008]. For that reason, a lime-based consolidant (i.e. lime-water) has been traditionally preferred due to its high compatibility and durability [Brajer and Kalsbeek, 1999; Baglioni et. al., 2014]. The consolidation of limewater ($Ca(OH)_2$ aqueous solution) is based on the carbonation reaction produced when portlandite ($Ca(OH)_2$) is exposed to open environments with CO_2 and H_2O giving rise to $CaCO_3$, which is the matrix of calcareous materials. However, this technique presents some important limitations such as the reduced impregnation depth and the very slow carbonation process, which in many cases leads to unsatisfactory treatments [Price et. al., 1988].

Nanolime dispersions were created to overcome the limitations of the lime-water technique. The consolidation effect of nanolime occurs by carbonation reaction in the same way as for lime-water. However, the smaller size of the lime particles improves the consolidation effectiveness as these are more reactive and reach greater penetration depths. The popularity of nanolime has been growing since its first synthesis in 2001. Both commercial nanolime products (Calosil® and Nanorestore®) have proven to be effective products for superficial consolidations (e.g. wall-paintings, stuccoes or plasters) [Otero et al, 2017; Baglioni et al, 2014]. In contrast, the results for consolidations deeper than a few millimetres of highly porous substrates are fewer and often controversial with some unsatisfactory results [Costa and Delgado-Rodrigues, 2012].

Nanolime effectiveness depends on several factors: i) external factors such as high Relative Humidity (~75%RH) clearly enhance the carbonation process of nanolime [Lopez-Arce et al, 2010]; ii) type of solvent can influence the deposition of the nanoparticles in the pores reducing the migration of the nanoparticles toward the surface during

solvent evaporation [Borsoi et al, 2016]; iii) concentration of nanolime can increase the deposition of particles in the pores [Arizzi et al, 2015] v) repetition of applications of low concentrated nanolime can increase the consolidation effectiveness of the treatment [Slikova et al, 2012]; vi) a content of water in the alcoholic solvent increases the carbonation process [Dei and Salvatori 2006; Daniele and Taglieri 2010; Daniele et al, 2018; Taglieri et al, 2017]; and vii) storage conditions of nanolime prior to application (low temperatures for short periods of time) reduces the conversion of calcium hydroxide into calcium alkoxides which clearly enhances the carbonation of nanolime [Rodriguez-Navarro et al, 2016].

Nanolime has been successfully synthetized by diols [Salvadori and Dei, 2001, Samanta et al., 2016], w/o microemulsions [Nanni and Dei, 2003], aqueous solutions [Sequeira et al, 2006, Daniele et al, 2012], solvothermal reactions [Poggi et al, 2016, Borsoi et al, 2016], plasma metal reaction method [Liu et al, 2010], or anion exchange kinetics [Volpe et al, 2016; Taglieri et al, 2015]. Synthetized nanoparticles present slightly different features in terms of reactivity and particle size depending on the synthesis route [Otero et al, 2018]. Nanolimes synthetized by solvothermal reactions present nanoparticles with sizes ranging from 100 to 300 nm, which usually form clusters of approximately 600 nm [Borsoi et al, 2016, Rodriguez-Navarro et al, 2013]. Conversely, nanolimes synthetized by anion exchange processes present nanoparticles with sizes ranging from 20 to 80 nm, which usually form clusters of approximately 200 nm [Taglieri et al, 2018].

The aim of this paper is to determine the influence of two nanolime products with different nanolime particle size and two substrates with different pore structure on the effectiveness of nanolime treatments. In this experiment, the consolidation effectiveness of two nanolimes with large difference in particle size onto two limestones with different pore size distribution have been investigated. The consolidation effectiveness was assessed by studying changes in porosity (MIP), water absorption capillarity (WAC), drying kinetics, drilling resistance (DRMS), superficial cohesion (STT) and aesthetic changes (colorimeter). The approach mimics that of a conservator faced with the conservation/restoration of a cultural heritage building/monument who needs to determine, with a minimum of testing, the most appropriate consolidation method [Rodriguez Delgado and Grossi, 2007].

2. Materials and methods

2.1 Limestone samples

Two limestones were used for the test:

- **Weathered limestone 1**: This sample, shown in Figure 1, is a weathered Doulting stone capital from the Wells Cathedral (Somerset, UK), a building listed as Grade I in the National Heritage List for England (NHLE) [Historic England, 2011]. This capital was removed from the Cathedral during a restoration intervention and was used by Prof. Clifford Price for a research experiment in the 1980s [Price, 1989; Doehne and Price, 2009]. In Price's experiment, the left-hand side (Fig. 1a) was treated with Brethane (a MTMOS based product) whilst the right-hand side was left untreated [Price, 1989]. After the experiment, the capital was stored in the Building Research Establishment (BRE) outdoor historic stone deposit (Watford, UK). In this research, only the untreated area which had not been treated with the Brethane was used. Doulting limestone is a clastic sedimentary rock composed of fragments of older Carboniferous limestones which were eroded and later re-deposited and cemented together [Price, 1989]. The rock can be classified as intramicrite [Folk, 1959] or grainstone [Dunham 1962]. This stone is referred to as CP. The capital was cut into 35 x 35 x 35 mm cubes for testing.

a)  b) 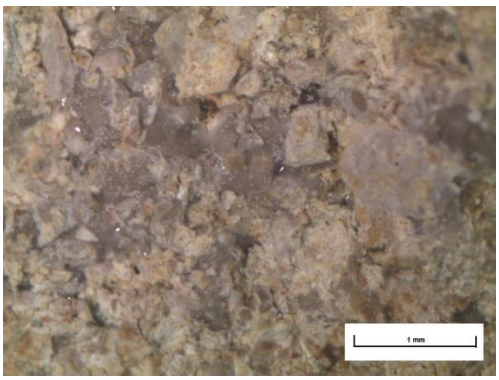

Figure 1. Weathered capital of Doulting stone (referred as CP) from the Wells Cathedral (UK). a) capital; b) stereomicroscope image of a fragment of Doulting stone

The elemental composition of this stone was determined by XRF (Philips PW2400) on pressed powder samples (Retsch PP-40 pellet press). XRF results shows that CP stone is composed of 93.4 (±0.2) of Ca, 2.00 (±0.09) of Si, 1.7 (±0.03) of S, 1.3 (±0.04) of P, 0.7 (±0.004) of Fe and 0.3 (±0.01) of K.

The mineralogical composition was determined by X-Ray Diffraction (PANalytical XPert PRO) where XRD patterns were recorded with a step size of 0.026˚2θ, in the angular range 20-70°2θ. The samples were ground and sieved through an 80 μm sieve mesh and placed over an XRD zero-background sample holder. X-ray data were fitted using the pseudo-Voigt profile function. Specimen displacement, polynomial coefficients for the background function, lattice parameters, profile parameters, and Gaussian and Lorentzian profile coefficients were refined [Bish and Post, 1989]. XRD refinement shows that Calcite ($CaCO_3$, ICSD #01-086-2334) is the only detected mineral in the stone, suggesting that other mineral phases (e.g. feldspar containing P, Si, Fe, K, Al and S, which were elements detected by XRF) could be present in amorphous or poorly crystallised phases or in amounts below the instrument detection limit (< 1%).

The pore structure was determined by Mercury Intrusion Porosimetry (MIP) by means of a PASCAL 140/240 instrument. The contact angle was taken to be 140°. Samples for MIP consisted of stone fragments measuring approximately 8x15 mm which were dried in a fan-assisted oven at 60 ºC until constant weight. MIP results shows that the porosity of this stone is 14.10 (±0.42) % and the density is 2.0801 (±0.03) g/cm^3.

- **Weathered limestone 2** (Fig. 2): The origin of this piece is unknown. The specimen was stored in the Building Research Establishment (BRE) outdoor historic stone deposit. It is a sedimentary rock composed of ooids cemented by sparry calcite. The rock can be classified as an intrasparite [Folk, 1959] or Grainstone [Dunham 1962]. The surface of the stone is covered by a dark grey patina (Fig. 2a). This stone is referred to as LS. This stone was also cut into 35 x 35 x 35 mm cubes for testing making sure that their surface was free of the dark grey patina.

a)  b) 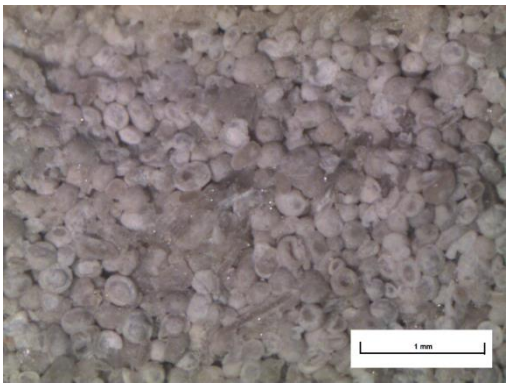

Figure 2. Weathered limestone (referred to as LS). a) Studied limestone showing a black patina on the surface; b) stereomicroscope image of the limestone.

The elemental composition of this stone was calculated by XRF which shows that LS stone is composed of 95.2 (±0.2) of Ca, 1.15 (±0.07) of Si, 1.3 (±0.03) of P, 0.9 (±0.03) of Fe, 0.5 (±0.2) of Al, 0.3 (±0.01) of S and 0.2 (±0.01) of K.

XRD refinement shows that Calcite (CaCO3, ICSD #01-086-2334) is the only detected mineral in this stone, suggesting that any other mineral phases (e.g. feldspar containing P, Si, Fe, K, Al and S, which were elements detected by XRF) could be present in amorphous or poorly crystallised phases or in amounts below the instrument detection level (< 1%).

The pore structure was determined by Mercury Intrusion Porosimetry (MIP) which showed that the porosity of this stone is 16.30 (±0.22) % and the density is 2.0354 (±0.05) g/cm^3. Due to the nature of its allochems (sub-spherical grains, i.e. ooids) and due to the sparitic cement not filling completely the intergranular spaces, this limestone is characterised by a higher amount of larger pores than the CP limestone (see section 3.1).

2.2 Nanolimes

Two nanolime dispersions were used for this test:

- Nanorestore Plus Propanol 5® (CSGI Consortium - University of Florence, Italy) [Nanorestore® Italian Patent No. FI/96/A/000255]: 5 g/L nanoparticles in 2-propanol. Particles are plate-like hexagonal $Ca(OH)_2$ nanoparticles regularly shaped with a particle size ranging from 100 to 300 nm [Baglioni et al, 2014]. This dispersion is referred to as NAN.

- Nanolime synthesised through the method developed by the University of L'Aquila [Taglieri et al, 2015]: 5 g/L nanoparticles in 50-50% W/A (water - 2-propanol). Particles are plate-like hexagonal $Ca(OH)_2$ nanoparticles regularly shaped with a particle size ranging from 20 to 80 nm [Taglieri et al, 2017]. This dispersion is referred to as LAQ.

LAQ was synthesized through an anionic exchanges process carried out at room temperature and ambient pressure by mixing under moderate stirring an anion exchange resin (Dowex Monosphere 550A OH by Dow Chemical) with an aqueous calcium chloride solution ($CaCl_2$ by Sigma-Aldrich), as described in literature [Taglieri et al, 2015, 2017]. The concentration of chlorides was monitored during the process using a Vernier Chloride Ion-selective Electrode CL-BTA. The decrease of chloride content during the synthesis was very rapid and the synthesis was stopped when the ion exchange process was completed (zero kinetic exchange), with a total reduction of chloride content of 99.82% and a residual chloride content of 29.4 mg/L. After the synthesis, 50% vol. of the supernatant water of the produced nanolime (W) was extracted through a pipette and replaced by 50% vol. of isopropanol, maintaining the concentration at 5 g/L. A characterization of morphology, reactivity and colloidal stability of both nanolimes can be found elsewhere [Otero et al, 2018].

2.3 Nanolime treatments

Four specimens of each stone (CP and LS) were treated with both nanolimes (NAN and LAQ). The treatment was carried out by brush in outdoor conditions. Both nanolime suspensions were agitated before the treatment. Treatments started two days after the nanolime synthesis of LAQ to increase their effectiveness [Rodriguez-Navarro et al, 2016]. Each nanolime was applied by brush on just one dry and clean surface of each limestone cube (35 x 35 x 35 mm), until the consolidant reached the opposite side of the sample. The application was stopped when no further absorption was observed (surface remained wet for a period of at least one minute). Then the samples were left to dry and retreated again after 24 hours. Samples were weighed before and after each application to obtain the amount of nanolime absorbed by each cube. The treatment was considered complete when each cube absorbed 500 mg of calcium hydroxide (approximately 100ml) which required approximately 30 consecutive days of application for each nanolime. Upon treatment completion, the samples were stored outdoor in a sheltered area for a period of 28 days (RH ≈ 60-80%, monitored by a humidistat). A set of untreated control samples was also stored in the same conditions.

2.4 Consolidation effectiveness

Following 28-day outdoor exposure, the limestones cubes were dried to constant mass at 60 ºC in a fan assisted oven and subsequently stored in a desiccator until testing.

In order to assess the degree of carbonation of the nanolime after 28 days in the pores, one of the treated cubes was split in half and a 1% phenolphthalein solution (70% ethanol - 30% water) [BRE, 1995] was immediately sprayed onto one of the internal faces. Phenolphthalein is a chemical compound ($C_{20}H_{14}O_4$) which is a well-known pH indicator which remain colourless for pH <8.2, while it turns to pink/purple colour in pH conditions higher than 9.8 [Lahdensivu, 2016]. For this application, due to the alkalinity of nanolime (pH ~ 12), it turns pink in basic solution (nanolime) and colourless in non-basic medium ($CaCO_3$).

Pore size distribution and open porosity were measured by MIP. Tests were carried out on two samples taken from the surface (up to a depth of 50 mm) of treated and compared to control samples.

Capillary absorption curves were obtained [EN 13755] and the water absorption coefficient (WAC) was calculated. Upon completion of this test, samples were immersed in water for 24 hours and apparent porosity was calculated at room atmosphere [ASTM C 67-00]. Their drying behaviour was also followed and the initial drying rate calculated [EN 16322]. This sequence was carried out on three control and three treated samples per each stone.

The influence of nanolime treatment on surface cohesion was evaluated by the 'Scotch Tape Test' (STT) according to ASTM, 2009 [ASTM D3359]. The test was carried out on treated and control samples with a mean of 9 measurements for each sample.

The resulting consolidation of both nanolimes was also evaluated by means of the Drilling Resistance Measurement System (DRMS) from SINT-Technology, regularly used in the literature for assessing consolidation effectiveness [Costa and Delgado-Rodrigues, 2012]. Tests were performed on both control and treated samples using drill bits of 5 mm diameter, rotation speed of 600 rpm, rate of penetration of 15 mm/min and penetration depth of 20 mm. Drilling resistance values were calculated as the mean of 6 tests per each treatment.

Any colour changes caused by treatments were evaluated with a spectrophotometer (Minolta CM508D Colorimeter) with the CIE-Lab system [Rodriguez-Navarro, 2013], using 30 readings taken in different areas per each treatment as well as of the control sample. Total colour variation (ΔE) is calculated by the formula:

$$\Delta E = \sqrt{\Delta L^{*2} + \Delta a^{*2} + \Delta b^{*2}}$$

where ΔL* is the change in luminosity (white-black parameter), Δa* (red-green parameters) and Δb* (blue-yellow parameters).

3. Results and Discussions

3.1 Consolidation effectiveness

The phenolphthalein test carried out on one of the internal faces of the cut open treated cubes shows that there is no Portlandite present in the pores following 28-day outdoor exposure. This result suggests that both nanolimes (NAN and LAQ) have fully carbonated in the pores in both stones after a period of 28 days at RH ≈ 60-80%.

The pore structure properties of treated and control samples for both stones are summarised in Table 1. MIP results show that all treated samples have lower porosity than the control. For the LS stone, both treatments obtained a similar porosity reduction. In the case of the CP stone, the NAN treatment yielded a higher porosity decrease than the LAQ. Both treatments also reduced the modal pore diameter while increasing the total pore surface area in both stones. LAQ treatments yielded a higher increase in total pore surface and decrease in modal pore diameter in both stones, which suggests that samples treated with LAQ present finer pore network than samples treated with NAN.

Table 1. Porosity properties of samples calculated by MIP

	Porosity (vol.%)	**Modal Pore diameter (μm)**	**Total pore surface area (m^2/g)**
LS-CO	17.90 (±0.21)	32.88 (±0.25)	0.801(±0.07)
LS-NAN	15.72 (±0.23)	32.10 (±0.21)	1.081 (±0.03)
LS-LAQ	15.51 (±0.19)	30.15 (±0.18)	1.433 (±0.05)
CP-CO	14.11 (±0.19)	34.47 (±0.27)	0.502 (±0.09)
CP-NAN	10.22 (±0.15)	13.52 (±0.17)	0.703 (±0.06)

CP-LAQ	12.83 (±0.29)	13.14 (±0.21)	1.867 (±0.06)

The pore size distributions of treated and control samples are shown in Figure 3. It is evident that both treatments affected the pore structure of the two stones. NAN appears to have filled the pores with larger diameters in both stones. In the case of the LS stone, which has a higher population of pores with diameter between 10 µm to 50 µm compared to CP, the NAN treatment also reduced the amount of pores with diameters between 10 and 40 µm (Fig 3a). Additionally, in this stone, MIP also recorded an increase of the pores with diameter between 40 to 100 µm. This is attributed to NAN reducing the number of pores with bigger diameters (>100 µm) which are outside of the measurement range of the used MIP technique. Moreover, as a result of this treatment, NAN caused a slight increase in the population of pores with diameters between 0.2 µm and 0.3 µm and between 0.01 µm and 0.03 µm. In the case of the CP stone, which presents a pore structure with large pores within the range 10-100 µm and intermediate pores between 0.1 to 6 µm, the treatment follows the same pattern. NAN treatment clearly closed the large pores with diameter between 20 and 100 µm, and in this case the treatment slightly reduced the amount of intermediate pores with diameters between 0.2 and 1 µm (Fig. 3b).

In contrast, MIP results show that LAQ treatment tends to fill both large and small pores alike. LAQ treatment appears to partially fill the pores causing in both stones an increase in the population of smaller pores. In the case of LS stone, LAQ treatment clearly closed large pores between 20 and 40 µm which is accompanied by an increase of the intermediate pores between 0.3 and 20 µm. This treatment also closed smaller sized diameter pores (0.06 to 0.3 µm) which is accompanied by an increase of the finer pores size distribution (0.01 to 0.06 µm) (Fig. 3c). In the case of CP stone, the treatment follows the same pattern. LAQ treatment filled the pores with large pore size distribution (11 to 100 µm) while increasing the amount of intermediate pores (2 to 11 µm) and closed the pores with diameter 0.1 to 2 µm while increasing the amount of finer pores (0.01 to 0.03 µm) (Fig. 3d).

These results suggest that the LAQ treatment could be more effective for consolidating fine pores in the range of 0.1 µm to 1µm, especially those < 0.6 µm, than NAN. This is attributed to the small particle size of LAQ (particle size ~20-80nm), which may allow a better penetration into pores with smaller size diameters when compared to NAN (particle size ~150-300nm). Moreover, nanoparticles tend to agglomerate and form clusters [Rodriguez-

Navarro et al, 2013; Borsoi et al, 2016; Rodriguez-Navarro et al, 2016]. The clusters measure approximately 600nm for NAN [Rodriguez-Navarro et al, 2013] and approximately 200nm for LAQ [Taglieri et al, 2017, 2018]. Thus, in the case of NAN, the access of the nanolime particles seems to be restricted to pores with large size diameter (> 600nm) while in the case of LAQ particles the access is also noticeable in pores with smaller size diameters up to 100nm. These results suggest that nanolimes with smaller particle size (e.g. LAQ) could be more effective for consolidation treatments of fine porous substrates (<0.6 µm) than other nanolimes (e.g. NAN) due to the smaller particle size and clusters.

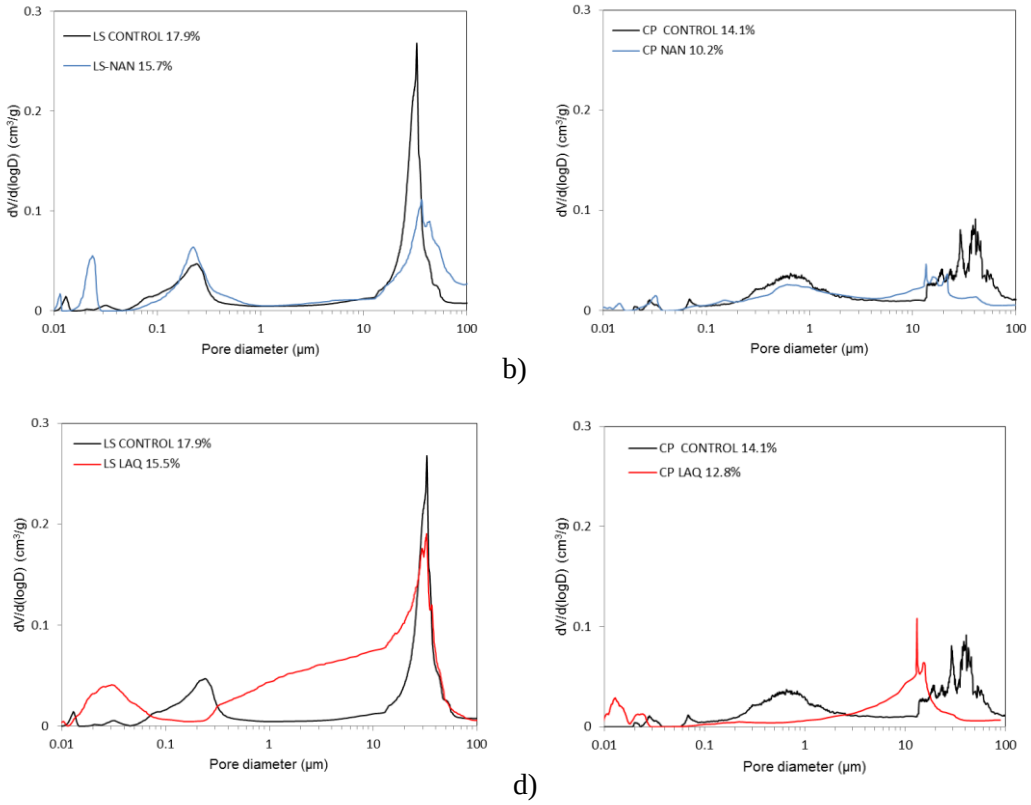

Figure 3. Pore size distribution of control and treated samples for: a) LS-NAN; b) CP-NAN; c) LS-LAQ; and d) CP-LAQ.

The water absorption and drying curves are reported in Fig 4 and Fig 5 and apparent porosity by immersion, water absorption and drying characteristics are reported in Table 2.

Table 2 shows that both nanolime treatments slightly reduced the apparent porosity of both stones. It also shows that the NAN treatment yielded a significant 77% decrease in the capillary absorption coefficient (WAC) in the LS limestone while LAQ only yielded a 15.8 % decrease in the same stone. This is attributed to the higher reduction of

the large pores following the NAN treatment without increasing the intermediate pores, which clearly slows down the capillary rise [Charola and Wendler, 2015]. In the case of CP stone, both treatments slightly reduced the water absorption by capillary coefficient and both presented similar curves to each other. All treatments yielded similar reduction of the total water absorbed by capillarity in both stones.

Table 2. Water absorption and drying characteristics

Parameter	LS-CO	LS-NAN	LS-LAQ	CP-CO	CP-NAN	CP-LAQ
Apparent Porosity (%)	7.48 (±0.13)	7.05 (±0.16)	6.96 (±0.21)	6.87 (±0.04)	5.99 (±0.13)	6.26 (±0.08)
W. absorption coefficient (10^{-3}g/cm^2 s$^{0.5}$)	27.4 (± 0.5)	6.1 (± 0.3)	23.1 (± 0.3)	13.9 (± 0.4)	13.2 (± 0.3)	13.8 (± 0.3)
W. absorbed at asymptotic value (g)	5.25 (±0.07)	5.17 (±0.08)	5.11 (±0.17)	4.12 (±0.11)	3.9 (±0.13)	4 (±0.09)
W. absorbed after 24-hour immersion (g)	5.55 ±0.13)	5.16 (±0.15)	5.18 (±0.21)	4.51 (±0.04)	4.01 (±0.13)	4.01 (±0.08)
Drying rate (10^{-3}g/ cm^3 h)	5.9 (±0.2)	5.8 (±0.4)	5.2 (±0.5)	4.4 (±0.10)	3.9 (±0.2)	3.7 (±0.3)
Time for total drying (h)	<50	<50	<50	<50	>50	>50

All treated stones took more time to reach the asymptotical values (Fig. 4). LS stone control samples reached the asymptotical values in the first 1.5 minutes of contact with water. In contrast, LS samples treated with LAQ needed 7 minutes and NAN treated samples needed over 2 hours. For the CP stone, both treated samples reached the asymptotical value in about 1 hour, which was only slightly higher than for the control samples.

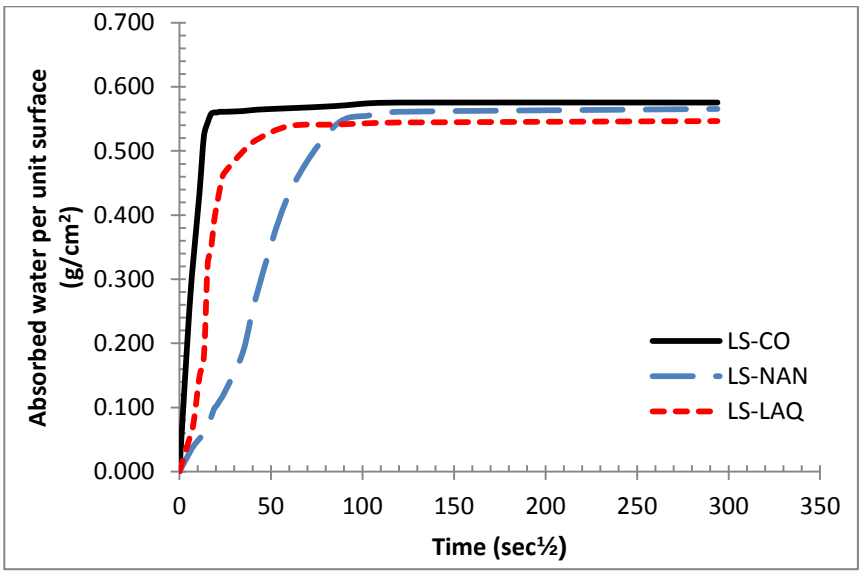

a)

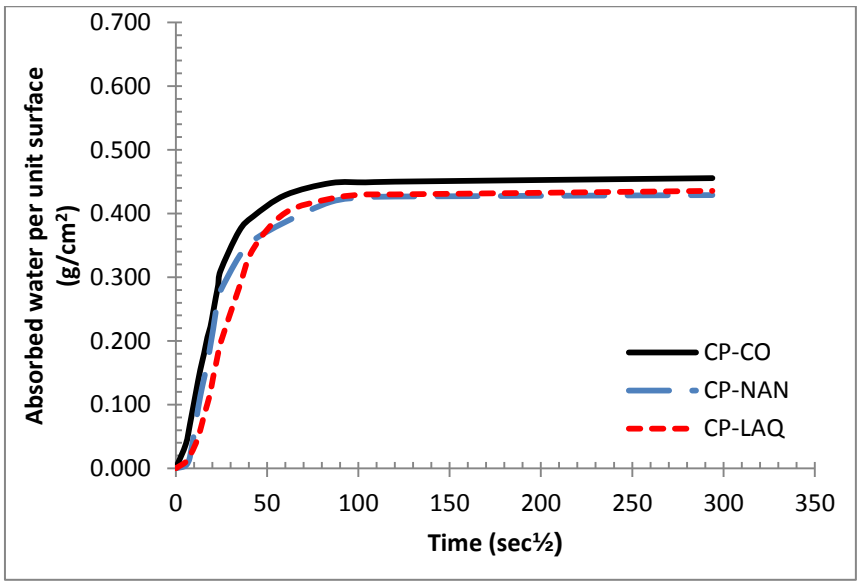

b)

Figure 4. WAC curves for a) LS; b) CP.

The drying curves for both stones are shown in Fig 5. Drying curves for LS and CP show that the treated samples take slightly more time to dry than control samples (Table 2). This is could be an undesirable behaviour should the difference increase as it would promote the risk of spalling when the stones are exposed to freeze-thaw cycles, or that of biological attack, etc [Charola et al, 2017]. The slower drying rate is attributed to the more compact pore structure in the weathered layer which has been consolidated after nanolime treatments. The denser structure reduces the liquid transport of water towards the surface hence slowing down the drying kinetics [Charola et al, 2017]. Both treatments present similar drying rate and total drying time to each other in both stones.

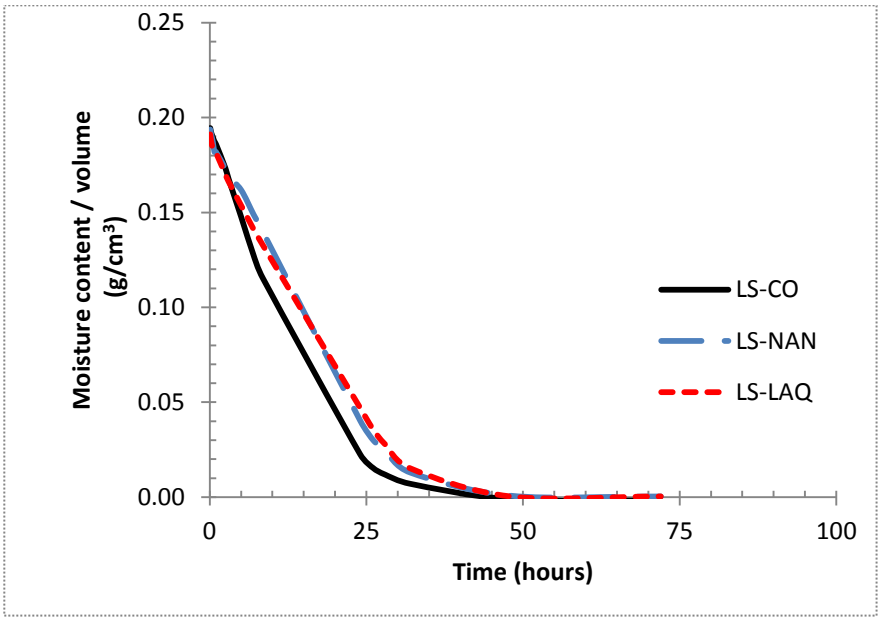

a)

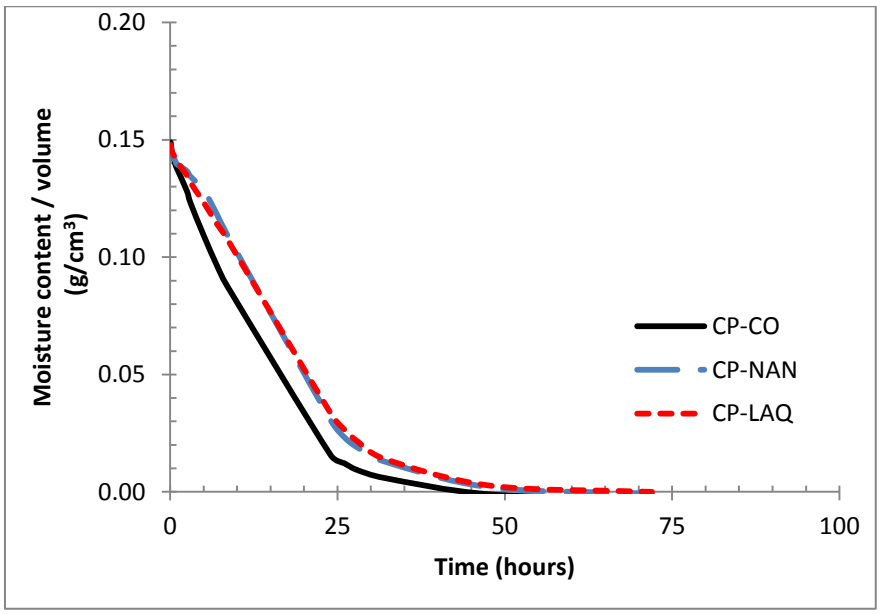

b)

Figure 5. Drying curves for treated samples of: a) LS limestone; b) CP limestone

The results of the Scotch Tape Test (STT) are shown in Table 3. All treatments obtained lower values of removed material after nanolime treatments (ΔW ≈ 62 - 88%). These results confirm that all surfaces are more compact after nanolime treatments. STT results confirm that the NAN treatment yielded the highest increase of surface cohesion in LS samples, which is in line with WAC and MIP results that show that this treatment is more effective in this type of stone and can be attributed to the higher reduction of the large pores. In contrast, LAQ treatment yielded the highest increase in the surface cohesion in CP samples suggesting that the surface is more compact for this stone following this treatment.

Table 3. Scotch Tape Test (STT) results

Code ID	Released material (mg/cm^2)	ΔW (%)	SD
LS-CO	9.94	-	6.4
LS-NAN	1.64	83.5	0.5
LS-LAQ	3.28	67.0	2.1
CP-CO	17.74	-	6.6
CP-NAN	6.67	62.4	7.6
CP-LAQ	2.04	88.5	1.4

Scotch area: 3 x 1.5 cm; SD (Standard Deviation of released material)

Drilling resistance results for both limestone samples are shown in Figure 6. The drilling resistance of LS limestone is constant throughout the drilling depth (20 mm). In contrast, the drilling resistance of CP limestone shows lower drilling resistance on the surface. This suggests that the external layer of this stone (Capital) has been affected by a

weathering process, which decreased the compactness of the stone at the surface. The average drilling resistance of CP stone is F ~ 12.5N (±2.59), lower than LS stone (F ~ 18N (±1.47). Both treatments significantly increased the drilling resistance in both stones. In the case of the LS stone (Fig 6a), the samples treated with NAN recorded the highest increase in drilling resistance (ΔF ~ 50%), which was more pronounced in the outer 14 mm. This is in line with STT, WAC results that shows this treatment is more effective reducing the superficial cohesion and reducing the water absorption by capillarity. In the same stone, LAQ treatment also yielded an increase in the drilling resistance (ΔF ~ 22.2%), which was constant throughout the drilling depth. The higher increase of strength of NAN in this stone is attributed to the higher reduction of the large pores (20-40 μm), as the reduction of large pores increases the mechanical strength more than in the case of a reduction in the number of small pores [Zhao et al, 2014]. In the case of CP stone (Fig. 6b), both treatments yielded similar drilling resistance which was constant throughout the drilling depth (20 mm). Both NAN and LAQ treatments resulted in a strengthening of the weathered layer, where the drilling resistance increases considerably in the outer 14 mm (ΔF ~ 20.8% for NAN and ΔF ~ 18.4% for LAQ).

DRMS results of both stones show that the penetration of the two nanolimes is significantly deeper in both limestones (14 – 20 mm) than previous studies on lime-mortars (6 - 10 mm) [Otero et al, 2018]. Furthermore, the increase in drilling resistance is significantly higher in pure calcite-based materials (both limestones, increase of ~10 - 20N) than in lime-mortars (increase of ~1N), which were composed of 82.3% quartz and 17.7% calcite [Otero et al, 2018]. The higher mechanical strength in lime-based substrates is attributed to the higher amount of calcite facilitating the bonding of the newly formed calcite to the existing calcite crystals thus inducing a higher resistance due to chemical compatibility [Lanas et al, 2004].

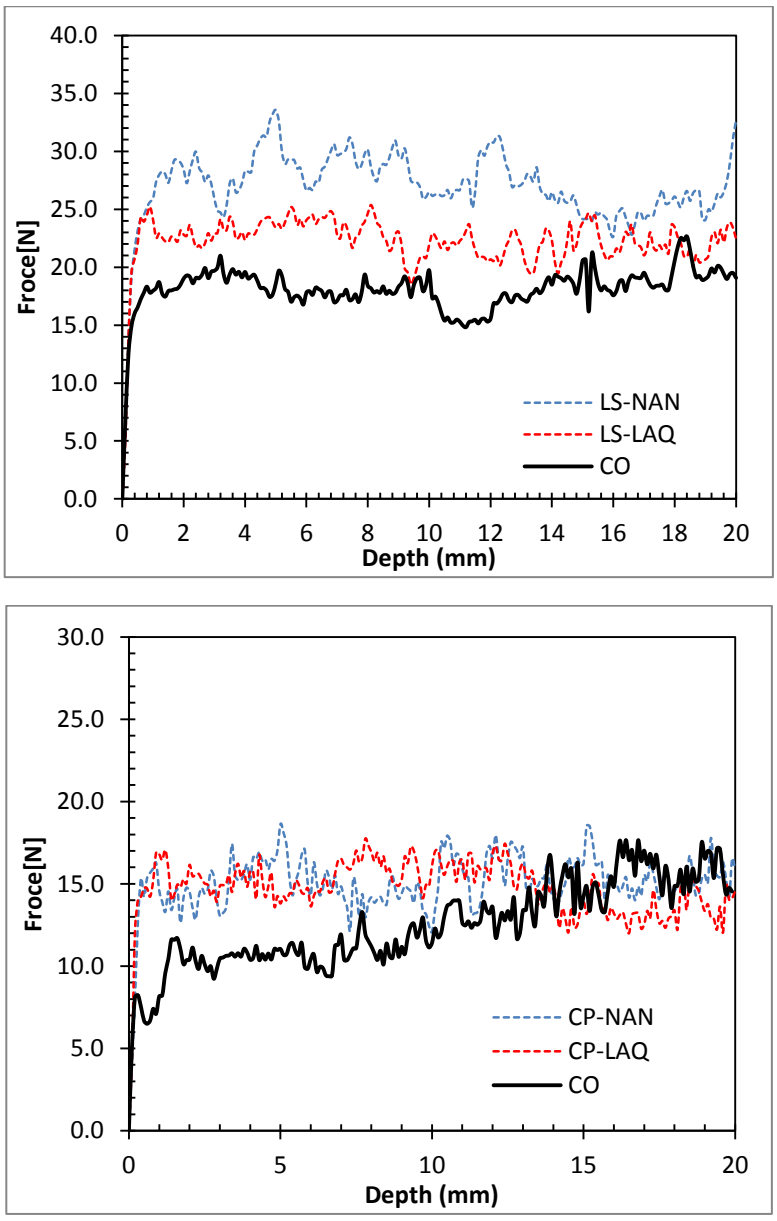

Figure 6. DRMS measurements of: a) limestone (LS); b) weathered capital (CP).

Ideally a consolidation treatment should improve the physico-mechanical properties without affecting the aesthetic properties. A common side effect of nanolime treatments is the whitening of the surface following treatment. Spectrophotometric analyses were carried out to measure changes in L* (white-black parameter) and ΔE* (total colour variations) following the treatments. ΔE* and ΔL* values <5 are considered suitable for consolidations as they are imperceptible by naked eye [Rodriguez-Navarro et al, 2013]. Results (Table 4) show that the treatments caused a whitening of the surface. Both treatments in both stones caused variations of both ΔE* and ΔL* with values above 5 and both obtained similar values to each other. The whitening is attributed to the accumulation of carbonated nanolime particles on the surface following the treatment.

Table 4. Chromatic alterations for treated samples

	ΔL*	Δa*	Δb*	ΔE*
LS-NAN	8.23 (±.098)	-1.76 (±0.67)	-6.79 (±0.89)	10.81
LS-LAQ	9.78 (±1.11)	-1.74 (±0.88)	-4.95 (±0.78)	11.09
-	-	-	-	-
CP-NAN	11.15 (±1.40)	-2.56 (±0.87)	-13.48 (±1.21)	17.68
CP-LAQ	10.28 (±1.52)	-0.61 (±0.56)	-4.43 (±0.87)	11.21

Mean Values determined on 30 measurements

4. Conclusions

The present study has shown that both nanolime products, NAN and LAQ applied by surface brushing, cause significant consolidation of two different types of limestones with diverse porosity structure. Both types of nanolime are considered acceptable for a potential in-situ consolidation treatment of weathered stone at the Cathedral of Wells or any historic structure built with Doulting stone. The consolidation effectiveness of both nanolimes present small differences depending on the substrate pore structure.

It has been shown that:

- Both treatments reduced the porosity of the two types of limestones. In the case of LS stone, both treatments obtained a similar porosity reduction. In the case of CP stone, the NAN treatment yielded a higher porosity decrease than the LAQ one. However, LAQ treatments yielded higher increase in total pore surface in both stones than NAN did, suggesting that LAQ treated samples present a finer pore network.

- The pore size distribution curves show that NAN treatment predominantly tends to close the pores with large pore sizes (~ 20 - 100µm), while LAQ treatment tends to fill both large (~20 - 100µm), and small pores (~0.07 – 2 µm) equally. These results suggest that LAQ treatment could be more suitable to consolidate substrates with finer pores than NAN and can be attributed to the smaller particle size of LAQ (~20-80nm) and smaller cluster formation (~200nm), compared to NAN particle size (~150-300nm) and clusters (~ 600nm)., that could facilitate the access of the nanoparticles to the finer pore structure (<0.6 µm).

- Both treatments reduce the water absorption by capillarity and drying rates due to the finer pore network in the stone's surface following treatment. NAN treatment yielded the largest decrease in capillary absorption rate for the LS limestone as this treatment yielded higher reduction of the large pores without increasing the intermediate pores. In the case of CP stone, both treatments reduced the water absorption by capillarity rate and both present similar water absorption curves.

- Scotch tape test confirms that both treatments successfully restore the surface cohesion of both limestones. NAN treatment yielded the highest increase in the surface cohesion in LS samples, where the treatment yielded higher reduction of the large pores.

- Both treatments clearly increase the drilling resistance of the stone after treatments. NAN treatment clearly yielded the highest increase of the drilling resistance ($\Delta F \sim 50\%$) in the LS stone, which is attributed to the increased filling of the large pores. However, in the CP stone, both treatments yielded a similar drilling resistance as both resulted in similar reduction of the large pores. Both treatments were able to consolidate the external weathered layer of the sample maintaining a constant drilling resistance throughout the stone. These results suggest that nanolime with larger particle size (e.g. NAN) could be more effective in coarse porous substrates as they yield higher reduction of the large pores (20-40 μm) and higher increase of mechanical properties than nanolimes with smaller particle size (e.g. LAQ).

- The penetration and increase of the drilling resistance due to nanolime treatments is significantly higher in pure calcite-based substrates (both limestones) than in lime-mortars composed of approximately 80% of quartz and 20% of calcite [Otero et al, 2018]. The higher mechanical strength can be attributed to the fact that the bonding between calcite-calcite delivers higher resistance due to its higher chemical compatibility [Lanas et al, 2004].

- Finally, colorimeter results show that both treatments caused a slight whitening of the surface of the limestones.

One conclusion of this study is that the selection of a nanolime product for a consolidation treatment must be done in relation with the nanolime particle size and the substrate pore structure. Thus, Nanorestore Plus IP5® would be more suitable for consolidating stones with large pore sizes and L'Aquila nanolime for stones with fine pore sizes. Further studies are required to better understand the influence of the particle size in relation to the substrate porosity.

Acknowledgements

This research has been funded by the Vice Chancellor's Scholarship within the Doctorate Program by Sheffield Hallam University (UK). Authors want to thank Prof. Clifford Price and Dr. Tim Yates from Building Research Establishment (BRE) their help to get the substrates. The authors declare that there is no conflict of interest and take a neutral position to offer an objective evaluation of the consolidation process.

References

Arizzi, A., Gomez-Villalba L. S., Lopez-Arce P., et al., (2015), "Lime mortar consolidation with nanostructured calcium hydroxide dispersions: the efficacy of different consolidating products for heritage conservation". European Journal of Mineralogy, 27(3), pp.311–323.

ASTM D3359-02: Standard Test Methods for Measuring Adhesion by Tape Test, (2002), ASTM International.

ASTM C 67-00: Standard Test Methods for Measuring Apparent Porosity at atmospheric pressure, (2000), ASTM.

Baglioni, P., Chelazzi D., Giorgi R., et al, (2014), "Commercial $Ca(OH)_2$ nanoparticles for the consolidation of immovable works of art". Applied physics. A, Materials science & Processing, 114(3), pp.723–732

Bish D. L. and Post J. E., (1989), Modern powder diffraction. Mineralogical Society of America, Crystal Reasearch & Technology, Washington. ISBN 0‐939950‐24‐3.

Borsoi, G., Lubelli B., Van Hees R. et al., (2016), "Effect of solvent on nanolime transport within limestone: How to improve in-depth deposition". Colloids and Surfaces A: Physicochemical and Engineering Aspects, 497, pp.171–181.

Brajer I. and Kalsbeek N., (1999), "Limewater absorption and calcite crystal formation on a limewater-impregnated secco wall-painting", Studies in Conservation vol. 44 (3), pp. 145–156.

BRE Digest 405, (1995), Phenolphthalein Test, HMSO and the Building Research Establishment (BRE).

Charola A. E. and Wendler E., (2015), "An overview of the water-Porous building materials interactions", Restoration of building and monuments Journal, vol. 21(2-3), pp. 55-63.

Charola A. E., Vicenzi E. P., Grissom C. A., et. al., (2017), "Composition and characteristics of Kasorta limestons on the exterior of the National Museum of the American Indian Building", pp.17-26. J.Sledge, A. E. Charola, P. T. DePriest and R. Koestler, eds. Conservation of the Exterior of the National Museum of the American Indian Building, Smithsonian Contributions to Museum Conservation, No. 6. ISSN 1949-2359.

Costa D., Delgado-Rodrigues J., (2012), "Consolidation of a porous limestone with nano-lime", in: G. Wheeler (Ed.), 12th International congress on the deterioration and conservation of stone, New York, pp. 10–19.

Daniele, V., Taglieri, G., (2010), "Nanolime suspensions applied on natural lithotypes: The influence of concentration and residual water content on carbonatation process and on treatment effectiveness". Journal of Cultural Heritage, 11(1), pp.102–106.

Daniele, V. and Taglieri, G., (2012), "Synthesis of $Ca(OH)_2$ nanoparticles with the addition of Triton X-100. Protective treatments on natural stones: Preliminary results". Journal of Cultural Heritage, 13(1), pp.40–46.

Daniele V., Taglieri G., Macera L., Rosatelli G., Otero J., Charola A. E., (2018), “Green approach for an eco-compatible consolidation of the Agrigento biocalcarenites surface”, Construction and Building Materials 186 pp.1188-1199.

Dei, L., and Salvadori, B., (2006), "Nanotechnology in cultural heritage conservation: nanometric slaked lime saves architectonic and artistic surfaces from decay". Journal of Cultural Heritage, 7(2), pp.110–115.

Delgado Rodrigues, J., and Gorssi, A. “Indicators and ratings for the compatibility assessment of conservation actions” Journal of Cultural Heritage, 8 (2007) pp.32-43.

Doehne E., Price C. A., (2009), "Stone Conservation: An Overview of Current Research", Research in conservation Series, Getty Conservation Institute, USA.

Dunham R. J., (1962), "Classification of carbonate rocks according to depositional texture. In Ham, W.E. classification of carbonate rocks", Am. Assoc. Petroleum Geologists Mem. 1 pp.108–121

EN 13755, (2008), The English Standard for Natural stone test methods. Determination of water absorption at atmospheric pressure.

EN 16322. (2013), The European Standard CEN - Conservation of Cultural Heritage - Test methods - determination of drying properties.

Ferreira-Pinto, A. P. and Delgado-Rodrigues J., (2008), "Hydroxylating conversion treatment and alkoxysilane coupling agent as pre-treatment for the consolidation of limestones with ethyl silicate". In Stone Consolidation in Cultural Heritage: Research and Practice; Proceedings of the International Symposium, Lisbon, 6-7 May 2008, ed. J. Delgado-Rodriguez and J. M. Mimoso, 41-52. Lisbon: LNEC (Laboratorio National de Engenheria Civil).

Folk R. L., (1959), "Practical petrographic classification of limestone", Am. Assoc. Pet. Geol. Bull. 43 (1) pp.1–38.

Historic England. "Wells Cathedral", (2011), PastScape. Retrieved 4 196971

ICOMOS, (1931), "Carta del Restauro", the First International Congress of Architects and Technicians of Historic Monuments, Athens.

ICOMOS, (1964), "The Venice Charter", International Charter for the Conservation and Restoration of Monuments and Sites.

Lahdensivu, J. (2016) Cement Concrete Composites Vol. 65, p 29.

Lanas J, Perez-Bernal M. A., Bell M. A. et al, (2004), "Mechanical Properties of hydraulic lime based mortars", Cement and Concrete Research 34 pp.2191-2201.

Liu, T., Zhu Y., Zhang X., et al., (2010), "Synthesis and characterization of calcium hydroxide nanoparticles by hydrogen plasma-metal reaction method". Materials Letters, 64(23), pp.2575–2577.

López-Arce, P., Gomez-Villalba L.S., Pinho L., et al., (2010), "Influence of porosity and relative humidity on consolidation of dolostone with calcium hydroxide nanoparticles: Effectiveness assessment with non-destructive techniques". Materials Characterization, 61(2), pp.168–184.

Nanni, A., Dei, L., (2003), "$Ca(OH)_2$ nanoparticles from W/O microemulsions". Langmuir, 19(13), pp.933–938.

Nanorestore®, CSGI Consortium - University of Florence, Italian Patent No. FI/96/A/000255, filed on 31/10/1996.

520 Otero J., Charola A. E., Grissom C. A., Starinieri V., (2017), “An overview of nanolime as a consolidation method
521 for calcareous substrates”, Ge-conservacion, vol. 11, pp.71-78.
522
523 Otero J., Starinieri V., Charola A. E., (2018), “Nanolime for the consolidation of lime mortars: a comparison of
524 three available products”, Construction and Building Materials, ISSN: 0950-0618, Vol: 181, pp. 394-407
525
526 Poggi, G., Toccafondi N., Chelazzi D., et al, (2016), "Calcium hydroxide nanoparticles from solvothermal reaction
527 for the deacidification of degraded waterlogged wood". Journal of Colloid and Interface Science, 473, pp.1–8.
528
529 Price, C., Ross, K., White, G., (1988), "A further appraisal of the ’Lime Technique’ for limestone consolidation,
530 using a radioactive tracer". IIC journal.Studies in Conservation, vol. 33 (4), pp.178–186.
531
532 Price, C., (1989), "Conservation de la Façade ouest de la cathedrale de Wells, In L'Ornementation architecturale en
533 pierres dans les monuments historiques: Chateau de Fontaineableau", October 1988. Actes des colloques de la
534 direction du Patrimoine, 1989, pp.38-40. Reviews consolidation of limestone with Alkoxysilanes and lime
535 treatments.
536
537 Rodriguez-Navarro C., Suzuki A., Ruiz-Agudo E., (2013), "Alcohol dispersions of calcium hydroxide
538 nanoparticles for stone conservation", Langmuir vol. 29, pp. 11457−11470.
539
540 Rodriguez-Navarro, C., Bettori I., Ruiz-Agudo E., (2016), "Kinetics and mechanism of calcium hydroxide
541 conversion into calcium alkoxides: Implications in heritage conservation using nanolimes", Langmuir, 32(20), pp.
542 5183-5194.
543
544 Salvadori, B., Dei, L., (2001), "Synthesis of $Ca(OH)_2$ nanoparticles from diols". Langmuir, 17(8), pp.2371–2374.
545
546 Samanta, A., Chanda D. K., Das P. S., et al., (2016), "Synthesis of nano calcium hydroxide in aqueous medium".
547 Journal American Ceramic Society, 795(37004), pp.787–795.
548
549 Sequeira, S., Casanova C., Cabrita E. J., (2006), "Deacidification of paper using dispersions of $Ca(OH)_2$
550 nanoparticles in isopropanol", Journal Cultural Heritage, 7, pp.264–272.
551
552 Slizkova Z., Frankeova D., (2012), "Consolidation of a porous limestone with nanolime". Proceedings of the 12th
553 International Congress on the Deterioration and Conservation of Stone, New York.
554
555 Taglieri, G., Daniele V. Del Re, et al, (2015), "A new and original method to produce $Ca(OH)_2$ nanoparticles by
556 using an anion exchange resin". Advances in Nanoparticles, 4, pp.17–24.
557

Taglieri G., Daniele V., Macera L., Mondelli C., (2017), Nano $Ca(OH)_2$ synthesis using a cost-effective and innovative method: Reactivity study, Journal of American Ceramic Society, 2017; pp.1-13; DOI: 10.1111/jace.15112.

Taglieri G., Otero J., Daniele V., et. al., (2018), "The biocalcarenite stone of Agrigento (Italy): Preliminary investigations of compatible nanolime treatments", Journal of Cultural Heritage, Vol. 30, pp 92-99.

Volpe R., Taglieri G., Daniele V., et. al., (2016), "A process for the synthesis of $Ca(OH)_2$ nanoparticles by means of ionic exchange resin", European patent EP2880101.

Wheeler G., (2005), "Alkoxysilanes and Consolidation of stone", Research in conservation Series, Getty Conservation Institute, USA.

Wheeler G., (2008), "Alkoxysilanes and the consolidation of stone: Where we are now. In Stone Consolidation in Cultural Heritage: Research and Practice", Proceedings of the International Symposium, Lisbon, 6-7 May 2008, ed. J. Delgado-Rodriguez and J. M. Mimoso, 41-52. Lisbon: LNEC (Laboratorio National de Engeneria Civil).

Zhao H., Xiao Q., Huang D., et al, (2014), Influence of Pore Structure on Compressive Strength of Cement Mortar, Scientific World Journal. 2014; 247058. DOI: 10.1155/2014/247058.